Synthesis and characterization of Cu_2O and CuO nanoparticles in distilled water using electrochemical process

S. Krobthong [a], K. Umma [b], T. Rungsawang [a], T. Mirian [a], S. Wongrerkdee [a,*], S. Nilphai [c,*], K. Hongsith [d], S. Choopun [d], S. Wongrerkdee [e], C. Raktham [f], P. Pimpang [g]

[a] *Department of Physical and Material Sciences, Faculty of Liberal Arts and Science, Kasetsart University Kamphaeng Saen Campus, Nakhon Pathom 73140, Thailand*

[b] *Department of Science, Faculty of Science and Agricultural Technology, Rajamangala University of Technology Lanna, Chiang Mai 50300, Thailand*

[c] *Physics Program, Department of Science and Technology, Faculty of Liberal Arts and Science, Roi Et Rajabhat University, Roi Et 45120, Thailand*

[d] *Department of Physics and Materials Science, Faculty of Science, Chiang Mai University, Chiang Mai 50200, Thailand*

[e] *Faculty of Engineering, Rajamangala University of Technology Lanna Tak, Tak 63000, Thailand*

[f] *Faculty of Education, Uttaradit Rajabhat University, Uttaradit 53000, Thailand*

[g] *Faculty of Science and Technology, Pibulsongkram Rajabhat University, Phitsanulok 65000, Thailand*

The synthesis of metal oxide semiconductors has garnered considerable attention due to their wide-ranging applications in fields such as electronics, optoelectronics, catalysis, and photovoltaics. This study presents the synthesis of copper oxide nanoparticles (NPs) in distilled water through a two-probe electrochemical process at varying applied voltages. The synthesized copper oxide NPs exhibited a color spectrum from light to dark brown, suggesting the formation of copper oxide in the distilled water. Preliminary observations utilizing the Tyndall effect with a red laser light confirmed the colloidal nature of the solution. Photoluminescence emissions highlighted the semiconducting properties of the synthesized copper oxide NPs. The copper oxide NPs exhibited small size into quantum dots (QDs) at lower applied voltages, whereas higher voltages produced larger sizes. The appearance of ring-like patterns suggested a polycrystalline structure, which was further corroborated by selected area electron diffraction analysis, confirming the crystalline structure of Cu_2O at low voltages and CuO at higher voltages. This study, therefore, demonstrates a straightforward method for synthesizing copper oxide using a two-probe electrochemical process, with the potential to produce QD and NP structures by modulating the applied voltage.

(Received October 14, 2024; Accepted January 8, 2025)

Keywords: Copper oxide, Electrochemical process, Nanoparticle, Quantum dot

1. Introduction

Metal oxide semiconductors (MOS) with notable conductive properties have been extensively studied for diverse applications. Copper oxide is a particularly interesting MOS, conventionally utilized in a wide range of fields, including sensors, catalysts, conductive materials, water purification systems, energy storage devices, antimicrobial agents, and photovoltaics [1]. Copper oxide enhances these applications' efficiency, accuracy, durability, and response time. However, the relatively large particle size of conventionally prepared copper oxide presents challenges in controlling specific properties. Reducing the size of nanostructured materials is

* Corresponding author: s.nilphai@reru.ac.th

https://doi.org/10.15251/DJNB.2025.201.13

crucial to improving these properties, primarily by increasing surface area, which enhances interfacial contact in various applications. Moreover, reducing the quantum dots (QDs) size significantly improves electronic properties due to quantum confinement effects.

Several methods for preparing MOS NPs are available, including precipitation, microwave irradiation, hydrothermal synthesis, photochemical techniques, and electrochemical processes [2-6]. For instance, chemical precipitation was used to synthesize copper oxide NPs using the green source *Tragia involucrata* L. for water purification [7]. The structural and optical properties were characterized using various analytical techniques, revealing CuO monoclinic structures with a particle size of 46 nm, Cu−O stretching vibrations, an energy band gap (E_g) of 1.40 eV, and surface areas of 7.80 m^2/g with a pore size of 1.42 nm. The degradation efficiency of the CuO NPs photocatalyst was 78% for rhodamine B degradation. Another study reported the preparation of CuO-ZnO nanocomposites (NCs) using an electrochemical discharge process [8]. A copper rod and zinc plate served as cathode and anode, respectively, immersed in different electrolytes (KOH, NaOH, and $NaNO_3$) for discharge at a constant voltage of 120 V. The average crystallite sizes were 14.33, 18.55, and 12.82 nm for NCs prepared in KOH, NaOH, and $NaNO_3$ electrolytes, respectively. The morphology exhibited various shapes, such as NPs, clusters, pencil-like nanorods (NRs), flowers, and rice-like structures. The E_g values were 3.06, 3.04, and 3.14 eV for NCs discharged in KOH, NaOH, and $NaNO_3$ solutions, respectively. Similarly, CuO/ZnO heterojunction nanorod arrays were synthesized via a photochemical method [9]. The deposition of a $Cu_2(NO_3)(OH)_3$/ZnO precursor was carried out by immersing ZnO NRs into a $Cu(NO_3)_2$ solution with UV irradiation, followed by annealing to form CuO/ZnO heterojunction structures. The transformation was complete at an annealing temperature exceeding 241.3 °C. A well-aligned (111) plane was detected, and good crystallinity with a plane distance of 0.232 nm was observed, indicating the presence of CuO, which was further confirmed by X-ray photoelectron spectroscopy. To achieve size reduction, the electrochemical process is an effective method for synthesizing a variety of NPs and QDs, such as CeO_2 QDs [10], reduced graphene QDs [11], CdSe QDs [12,13], nitrogen-doped carbon QDs [14], and MoS_2 QDs [15]. The electrochemical process offers simplicity, scalability, and flexibility in tuning particle size by adjusting synthesis parameters such as applied voltage, electrolyte type, and concentration. Additionally, it is a cost-effective method requiring minimal initial resources.

This study aims to synthesize copper oxide using a homemade two-probe electrochemical process in distilled water electrolytes. The goal is to produce copper oxide in small sizes by modulating the applied voltage. The synthesized copper oxide QDs were characterized by their scattering behavior, absorbance, photoluminescence (PL) emission, morphology, size, and selected area electron diffraction (SAED) patterns. This approach highlights the electrochemical process's potential to produce flexible and controllable copper oxide with tailored properties.

2. Experimental details

Pure copper rods, measuring 7 cm in length and 3 mm in diameter, were prepared by initially cleaning them in acetone via ultrasonication for 20 minutes. The rods were then subjected to repeated sonication in a solution of isopropanol and distilled water (1:1 volumetric ratio) for an additional 20 minutes. Subsequently, the rods were dried using a nitrogen air gun. Two copper rods were then immersed in a beaker containing 30 mL of distilled water, ensuring a constant separation of 2 cm between the electrodes. Copper oxide NCs were synthesized through a homemade two-probe electrochemical process by applying 2, 5, 10, 15, 20, and 25 V voltages, with each condition maintained for 6 hours. Following the synthesis, the distilled water containing the copper oxide was collected and stored in a glass bottle for further analysis.

The synthesized copper oxide was characterized using multiple techniques. The Tyndall effect was initially examined using a red laser to observe scattering behavior. A UV-Vis spectrophotometer (Varian, Cary 50, Xenon flash lamp) was employed to measure the absorbance spectra. The measurements were taken across a wavelength range of 200–1000 nm with a resolution of 1.0 nm. Photoluminescence spectroscopy (Horiba Scientific, FluoroMax+ SpectroFluorometer, ozone-free xenon arc lamp) was conducted to study excitonic emission

behavior. Excitation was performed at 280 and 320 nm wavelengths, with emission wavelengths monitored over a wide range of 300–750 nm at a resolution of 1 nm. Particle sizes were determined using transmission electron microscopy (TEM; JEOL, JEM-2100Plus), and the images were analyzed with Image-J software [16]. Additionally, selected area electron diffraction (SAED) patterns were analyzed to determine the crystallographic structure.

3. Results and discussion

The photograph of copper oxide synthesized in distilled water for 6 hours using an electrochemical process at voltages ranging from 2 to 25 V was presented in Fig. 1(a). A noticeable color-change in the solution, from light to dark brown, occurs as the applied voltage increases. This color shift is a key indicator of changes in the size, concentration, and distribution of copper oxide particles. Preliminary investigations into the light scattering behavior of the copper oxide were conducted using the Tyndall effect, with a red laser light source, as depicted in Fig. 1(b). The observed intensities of the laser beam increased with higher applied voltages, suggesting that the degree of scattering was influenced by the voltage, which caused the greater the number of scattering centers, copper oxide colloids [17]. The color variation of colloidal suspension for synthesized copper oxide in distilled water suggests changes in the concentration or particle size of the copper oxide in the distilled water. It is well-known that in a pure solution, no scattering occurs as there are no particles to obstruct the light path. Conversely, the colloids act as scattering centers in a colloidal solution, altering the light path and rendering the beam's trajectory visible according to the Tyndall effect observation. These observations suggest that the synthesized copper oxide forms a colloidal suspension in distilled water [18], and the intensity of the observed laser beam increases slightly at higher applied voltages, indicating enhanced scattering. The electrochemical process used to synthesize the copper oxide was voltage-dependent, meaning that higher applied voltages likely increase the rate of particle formation or influence the oxidation state, morphology of the particles, and optical characteristics.

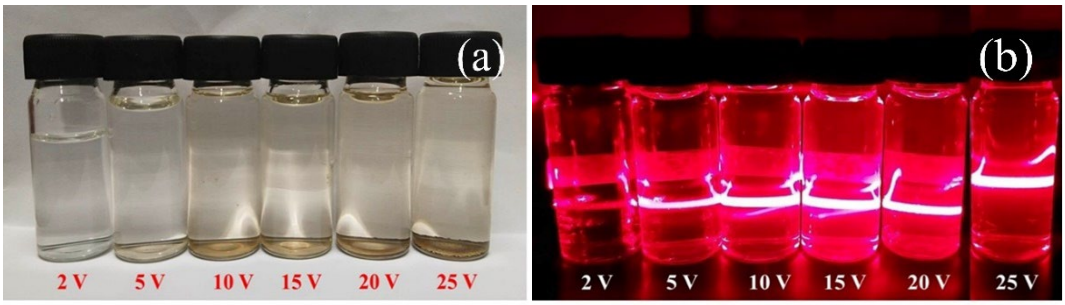

Fig. 1. Optical image of colloidal suspension of synthesized copper oxide in distilled water at different applied voltages: (a) without and (b) with laser beam irradiation.

The absorbance spectra of copper oxide in distilled water were presented in Fig. 2, measured over a wavelength range of 200–1000 nm. The absorbance spectra exhibited similar patterns for all samples, with variations in intensity. The increase in absorbance intensity with increasing applied voltage indicated that the voltage could control the synthesis conditions, directly influencing the optical properties of the copper oxide. This is a critical observation in colloidal chemistry that can influence the optical properties of the colloidal system in accordance with larger scattering beam in the Tyndall effect. Notably, for the sample at an applied voltage of 25 V, a significant increase in absorbance intensities was observed in the 200–400 nm range. This wavelength region corresponds to the UV-visible spectrum, where smaller particles typically exhibit stronger absorbance due to surface plasmon resonance and electronic transitions [19-21].

The enhanced absorbance in this region suggests that the synthesized copper oxide at higher voltages not only has a greater concentration of copper oxide particles but also includes smaller particles or a homogeneous distribution of particles that exhibit more pronounced optical effects at shorter wavelengths [22].

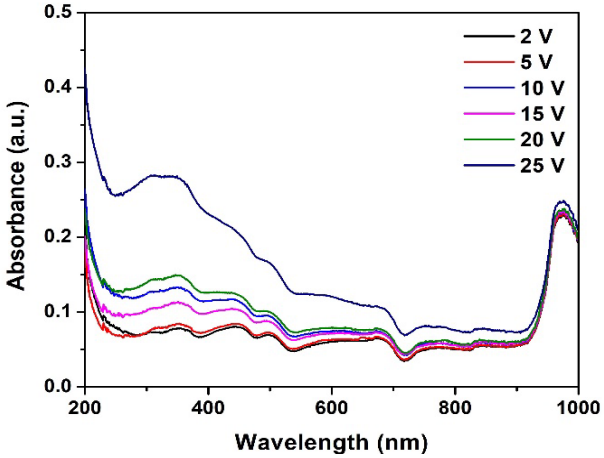

Fig. 2. Absorbance of synthesized copper oxide in distilled water at different applied voltages.

To further understand the excitonic emission of copper oxide, photoluminescence (PL) was analyzed under excitation wavelengths of 280 nm and 320 nm, as illustrated in Fig. 3. PL is a valuable technique for studying the optical properties of materials, providing insight into electronic transitions and the E_g of a material. In this case, the PL emission spectra for the two excitation wavelengths demonstrated similar patterns, with no significant differences between the two excitation conditions, as summarized in Table 1. The PL emission peaks occurring between 393 and 401 nm, which aligns with the expected emission from copper oxide [23]. The analysis revealed that the copper oxide synthesized at an applied voltage of 2 V exhibited the highest PL peak intensities. The PL intensity is often directly related to the characteristics of materials, as well as the concentration of excitons (electron-hole pairs) that recombine to emit light [24]. The exploration of the strongest PL emission peaks at a low applied voltage of 2 V suggests a high recombination rate due to quantum confinement [7] in the copper oxide which is the nature of small and independent particles. On the other hand, lower PL emission intensities were observed at higher applied voltages. The red-shift behavior in PL emission peaks at higher voltages implies more defects, possibly due to copper oxide aggregation caused by accelerated nucleation under high applied voltage.

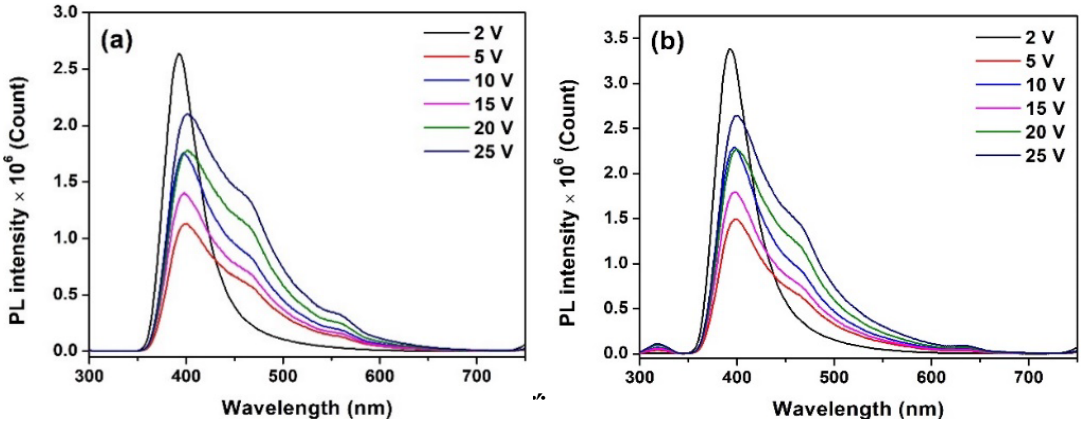

Fig. 3. PL emission spectra of copper oxide in distilled water at different applied voltages under excitation wavelength of (a) 280 nm and (b) 320 nm.

Table 1. PL emission peak wavelengths of copper oxide.

Applied voltage)V(	PL emission peak wavelength)nm(	
	Excitation at 280 nm	Excitation at 320 nm
2	393	393
5	399	398
10	397	399
15	397	398
20	401	400
25	401	393

High-resolution transmission electron microscopy (HR-TEM) was used to analyze the size of the synthesized copper oxide, as shown in Fig. 4. Samples synthesized at 5 V, 15 V, and 20 V were selected to represent low, medium, and high applied voltages, respectively. HR-TEM images revealed very small, spherical structures [25], with well-distributed dots at 5 V, while larger, irregular shapes were observed at 15 V and 20 V. Image-J software was used for size measurement, and the size distribution was plotted, as shown in Fig. 5. Copper oxide synthesized at 5 V had an average size of 1.79 ± 0.41 nm, classifying it as quantum dots (QDs) [12,26]. The spherical morphology and narrow size distribution observed at 5 V indicate the well-controlled nucleation and growth processes, which prevent the aggregation and promote the formation of uniform small particle sizes. In contrast, the particle sizes increased to 6.26 ± 2.28 nm and 5.85 ± 2.02 nm at applied voltages of 15 V and 20 V, respectively, resulting in a lower surface area compared to the condition at 5 V. These larger particles indicate that the synthesis process at high voltages causes rapid particle aggregation and growth. The particle size analysis implies that copper oxide with small size can be synthesized at lower voltages, while larger sizes form at higher voltages. The crystalline structures of copper oxide were examined using selected area electron diffraction (SAED) patterns to investigate phase formation, as shown in Fig. 6. The SAED patterns revealed ring-like structures for all samples, indicating polycrystalline nature [27-29], for the synthesized copper oxide QDs This polycrystalline structure is characteristic of materials synthesized through electrochemical processes due to rapid nucleation and random growth direction, resulting in multiple crystallization. Detailed analysis identified the crystalline structures of Cu_2O (JCPDs no. 5-0667) at lower voltages (5 V). The Cu_2O is typically formed under milder synthesis conditions and is associated with smaller particle sizes, which aligns with the QD formation observed at this voltage. For the high applied voltage of 15 V and 20 V, the crystalline phase shifted to CuO (JCPDs no. 48-1548). CuO formation is favored under extreme electrochemical conditions because higher voltages promote the oxidation of copper to its higher oxidation state (Cu^{2+}). The phase transformation of Cu_2O to CuO with increasing voltage correlates with the observed larger particle size and irregular morphology, as CuO tends to form larger and more complex structures in comparison with Cu_2O [30]. Thus, the low and high applied voltages result in crystalline structures of Cu_2O and CuO, respectively. This finding demonstrates the controllable synthesis of Cu_2O and CuO through the adjustment of applied voltage using a simple two-probe electrochemical process. The presence of both phases at different voltage levels demonstrates the versatility of the electrochemical process in tuning the material properties of copper oxide.

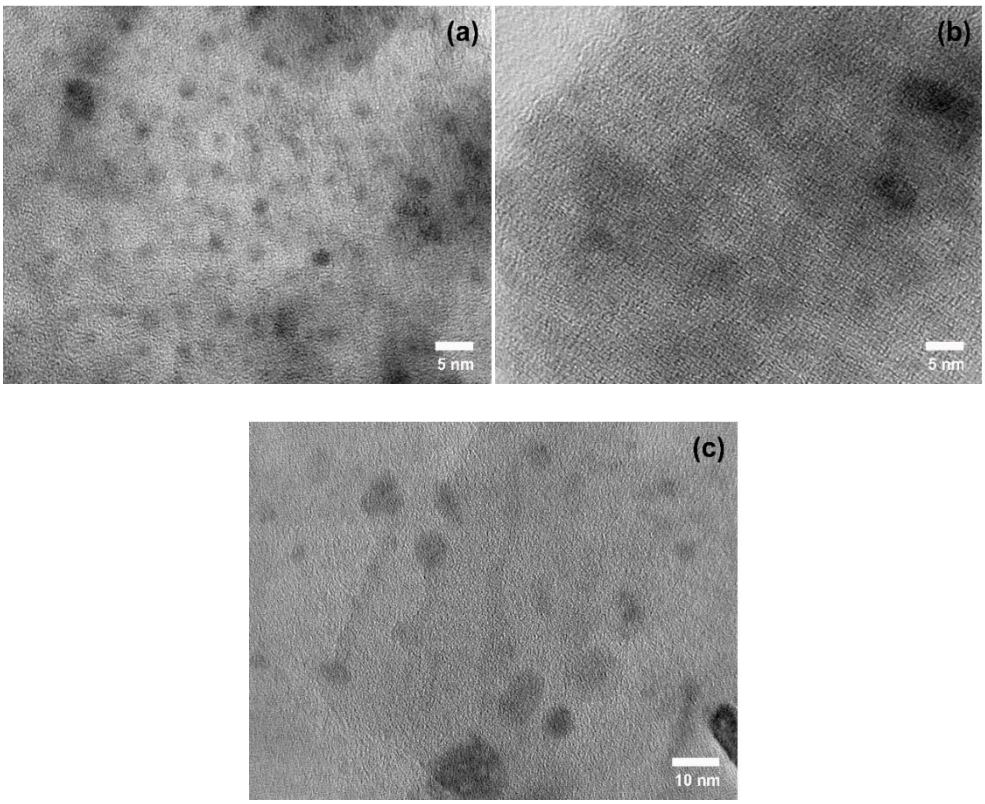

Fig. 4. HR-TEM images of copper oxide for applied voltages of (a) 5 V, (b) 15 V, and (c) 20 V.

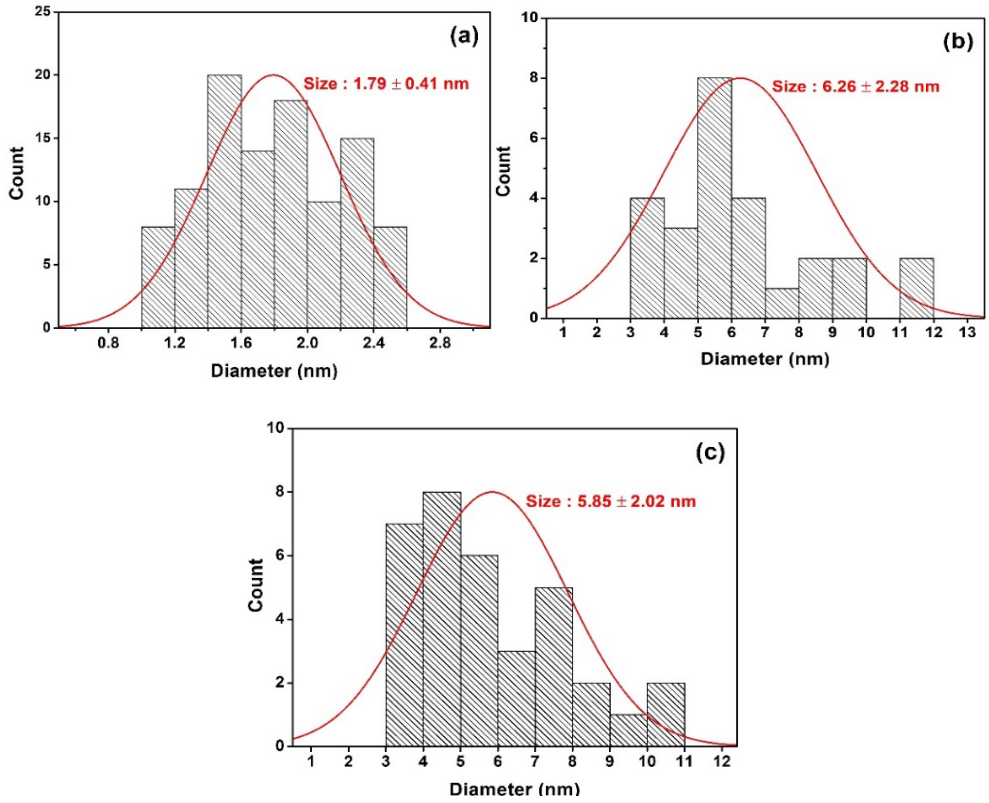

Fig. 5. The diameter of copper oxide for applied voltages of (a) 5 V, (b) 15 V, and (c) 20 V.

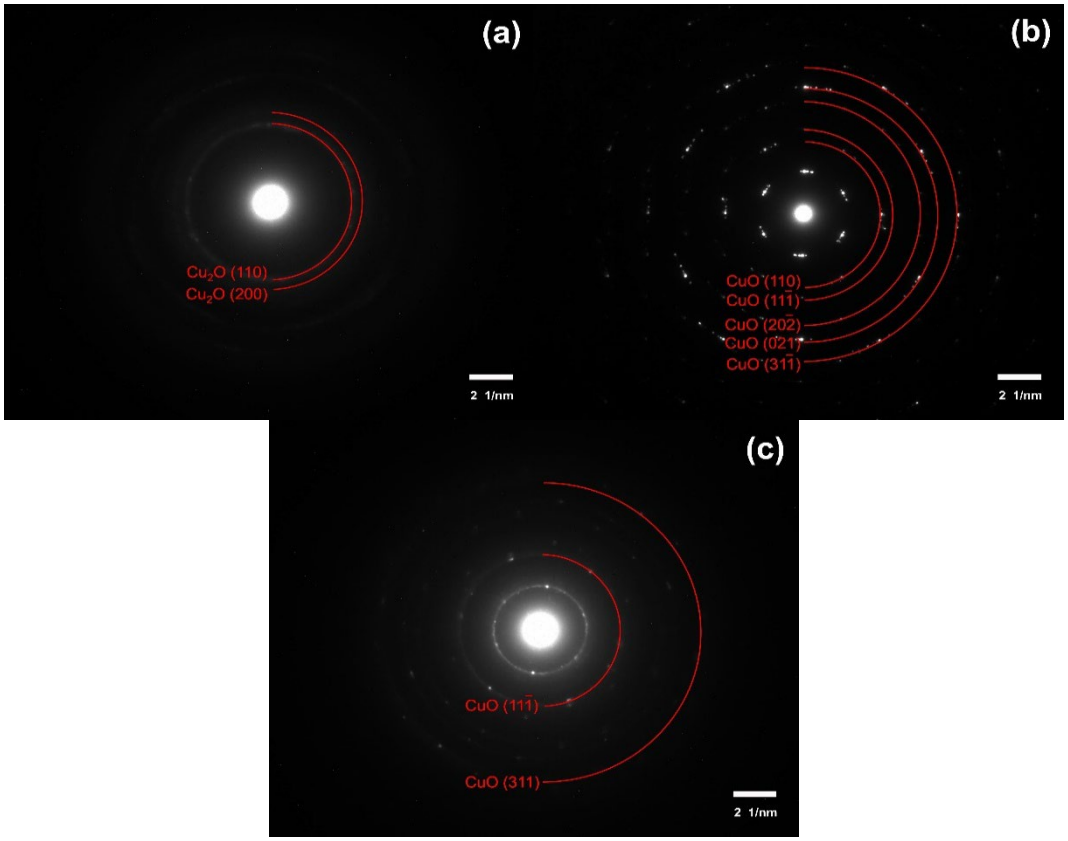

Fig. 6. SAED patterns of copper oxide for applied voltages of (a) 5 V, (b) 15 V, and (c) 20 V.

4. Conclusion

The copper oxide synthesized via a homemade two-probe electrochemical process in distilled water displayed a color shift from light to dark brown, corresponding to different applied voltages. Based on the Tyndall effect using a red laser light source, preliminary scattering observations confirmed that the copper oxide formed colloidal suspensions. The absorbance spectra exhibited similar patterns across samples, though with varying intensities. Photoluminescence emissions further verified the semiconducting properties of the copper oxide. HR-TEM analysis revealed an average particle size of 1.79 ± 0.41 nm at the lower applied voltage of 5 V, with larger particle sizes observed at higher voltages. This result indicates that the size of copper oxide QDs correlates directly with the applied voltage. SAED patterns exhibited ring-like structures, suggesting the polycrystalline nature of the synthesized copper oxide. Crystalline phase analysis identified Cu_2O at low voltages and CuO at higher voltages. The study demonstrates that a simple two-probe electrochemical process can be used to synthesize Cu_2O and CuO QDs, with tunable sizes based on the applied voltage. The ability to produce QD structures at lower voltages may be advantageous for quantum confinement applications.

Acknowledgments

This work was funded by the Faculty of Liberal Arts and Science, Kasetsart University Kamphaeng Saen Campus (Grant no. 306/2567). This work was also partially supported by Applied Physics Research Laboratory (APRL), Department of Physics and Materials Science, Faculty of Science, Chiang Mai University.

References

[1] E. C. Nwanna, T. C. Jen, Materials Science and Engineering: B **303**, 117333 (2024). https://doi.org/10.1016/j.mseb.2024.117333
[2] S. Moungsrijun, S. Wongrerkdee, Suranaree Journal of Science and Technology **29**(6), 030085 (2022).
[3] R. Panyathip, T. Sintiam, S. Weerapong, A. Ngamjarurojana, P. Kumnorkaew, S. Choopun, S. Sucharitakul, Surface Review and Letters **28**(12), 2150117 (2021). https://doi.org/10.1142/S0218625X21501171
[4] N. Patra, G. Ravi, ChemistrySelect **9**(18), e202400042 (2024). https://doi.org/10.1002/slct.202400042
[5] R. Rajamohan, C. J. Raorane, S. C. Kim, Y. R. Lee, Materials **16**(1), 217 (2023). https://doi.org/10.3390/ma16010217
[6] T. Sintiam, N. Saranrom, S. Phadungdhitidhada, S. Choopun, S. Sucharitakul, Journal of Physics: Conference Series **2431**, 012054 (2023); https://doi.org/10.1088/1742-6596/2431/1/012054
[7] M. Jeevarathinam, I. V. Asharani, Scientific Reports **14**, 9718 (2024). https://doi.org/10.1038/s41598-024-60008-7
[8] H. Bishwakarma, A. Kumar Das, P. Kumar, P. Kumar Singh, M. M Awad, Journal of Taibah University for Science **17**(1), 2188017 (2023); https://doi.org/10.1080/16583655.2023.2188017
[9] J. Li, T. Zhao, M. M. Shirolkar, M. Li, H. Wang, H. Li, Nanomaterials **9**(5), 790 (2019); https://doi.org/10.3390/nano9050790
[10] A. Younis, D. Chu, X. Lin, J. Yi, F. Dang, S. Li, ACS Applied Materials and Interfaces **5**(6), 2249-2254 (2016); https://doi.org/10.1021/am400168m
[11] R. Mohammad-Rezaei, J. Abbas-Zadeh, M. Golmohammadpour, E Hosseinzadeh, Electroanalysis **33**(12), 2428-2436 (2011); https://doi.org/10.1002/elan.202100256
[12] Y. Aniskevich, A. Antanovich, A. Prudnikau, M. V. Artemyev, A. V. Mazanik, G. Ragoisha, E. A. Streltsov, The Journal of Physical Chemistry C **123**(1), 931-939 (2019); https://doi.org/10.1021/acs.jpcc.8b10318
[13] Z. Bai, M. Chang, M. Peng, P. Liu, A. Lu, Z. Zhang, S. Qin, Journal of Luminescence **215**, 116614 (2019); https://doi.org/10.1016/j.jlumin.2019.116614
[14] G. Muthusankar, R. Sasikumar, S. M. Chen, G. Gopu, N. Sengottuvelan, S. P. Rwei, Journal of Colloid and Interface Science **523**, 191-200 (2018); https://doi.org/10.1016/j.jcis.2018.03.095
[15] J. Dong, X. Zhang, J. Huang, S. Gao, J. Mao, J. Cai, Z. Chen, S. Sathasivam, C. J. Carmalt, Y. Lai, Electrochemistry Communications **93**, 152-157 (2018); https://doi.org/10.1016/j.elecom.2018.07.008
[16] T. Rungsawang, S. Krobthong, K. Paengpan, N. Kaewtrakulchai, K. Manatura, A. Eiad-Ua, C. Boonruang, S. Wongrerkdee, Radiation Physics and Chemistry **223**, 111924 (2024); https://doi.org/10.1016/j.radphyschem.2024.111924
[17] M. A. Davydov, A. N. Fedorov, L. L. Chaikov, A. F., Bunkin, V. B. Oshurko, S. M. Perhsin, Optics and Laser Physics **113**, 423-427 (2021); https://doi.org/10.1134/S0021364021070055
[18] B. Bathula, T. R. Gurugubelli, J. Yoo, K. Yoo, Catalysts, **13**(4), 765 (2023); https://doi.org/10.3390/catal13040765
[19] V. Amendola, R. Pilot, M. Frasconi, O. M. Maragò, M. A. Iatì, Journal of Physics: Condensed Matter **29**(20), 203002 (2017); https://doi.org/10.1088/1361-648X/aa60f3
[20] H. M. E. Azzazy, M. M. H. Mansour, T. M. Samir, R. Franco, Clinical Chemistry and Laboratory Medicine, **50**(2), 193-209 (2023); https://doi.org/10.1515/CCLM.2011.732
[21] X. Fan, W. Zheng, D. J. Singh, Light: Science and Applications **3**, e179 (2014); https://doi.org/10.1038/lsa.2014.60
[22] F. Anjum, M. Shaban, M. Ismail, S. Gul, E. M. Bakhsh, M. A. Khan, U. Sharafat, S. B. Khan, M. I. Khan, ACS Omega **8**(20), 17667-17681(2023); https://doi.org/10.1021/acsomega.3c00129
[23] G. Sreedevi, K. Srinivas, M. Subbarao, S. Cole, Journal of Molecular Structure **1222**(1),

128903 (2020); https://doi.org/10.1016/j.molstruc.2020.128903
[24] K. Abiedh, Z. Zaaboub, F. Hassen, T. David, L. Sfaxi, H. Maaref, Applied Physics A **126**, 491 (2020); https://doi.org/10.1007/s00339-020-03654-8
[25] S. Krobthong, T. Rungsawang, N. Khaodara, N. Kaewtrakulchai, K. Manatura, K. Sukiam, D. Wathinputthiporn, S. Wongrerkdee, C. Boonruang, S. Wongrerkdee, Toxics **12**(3), 165 (2024); https://doi.org/10.3390/toxics12030165
[26] H. Park, D. J. Shin, J. Yu, Journal of Chemical Education **98**(3), 703-709 (2021); https://doi.org/10.1021/acs.jchemed.0c01403
[27] S. Krobthong, T. Rungsawang, S. Wongrerkdee, Toxics **11**(3), 266 (2023); https://doi.org/10.3390/toxics11030266
[28] S. Sujinnapram, S. Krobthong, S. Moungsrijun, C. Boonruang, N. Kaewtrakulchai, A. Eiad-Ua, K. Manatura, S. Wongrerkdee, Materials Today Communications **40**, 109501 (2024); https://doi.org/10.1016/j.mtcomm.2024.109501
[29] S. Wongrerkdee, S. Wongrerkdee, C. Boonruang, S. Sujinnapram, Toxics **11**(1), 33 (2023); https://doi.org/10.3390/toxics11010033
[30] E. Arulkumar, S. Thanikaikarasan, N. Tesfie, Journal of Nanomaterials **2023**, 8987633 (2023); https://doi.org/10.1155/2023/8987633